Role of the Head−to−Tail Overlap Region in Smooth and Skeletal Muscle β−Tropomyosin †

ARTICLE *in* BIOCHEMISTRY · FEBRUARY 2008

Impact Factor: 3.02 · DOI: 10.1021/bi701144g · Source: PubMed

Role of the Head-to-Tail Overlap Region in Smooth and Skeletal Muscle β-Tropomyosin†

Arthur T. Coulton,‡ Kezia Koka,‡ Sherwin S. Lehrer,§ and Michael A. Geeves*,‡

Department of Biosciences, University of Kent, Canterbury CT2 7NY, U.K., and Cardiovascular Program, Boston Biomedical Research Institute, Watertown, Massachusetts 02472-2829

Received June 11, 2007; Revised Manuscript Received October 24, 2007

ABSTRACT: Tropomyosin (Tm) is an α-helical, parallel, two-chain coiled coil which binds along the length of actin filaments in both muscle and non-muscle cells. Smooth and skeletal muscle Tms differ extensively at the C-terminus encoded by exon 9. Replacement of the striated muscle specific exon 9a-encoded C-terminus with that encoded by exon 9d expressed in smooth muscle and non-muscle cells increases the affinity of unacetylated α-SkTm for actin [Cho, Y. J., and Hitchcock-Degregori, S. E. (1991) *Proc. Natl. Acad. Sci. U.S.A. 88*, 10153−10157]. Here we show that swapping 10 amino acids at the C-terminus of β-SkTm with the corresponding 10 amino acids of β-SmTm had little effect on the regulation of S1 binding to actin, but Tm viscosity, Tm binding to actin, and troponin T_1 binding to Tm all become like smooth rather than SkTm. β-SkTm point mutations show that these properties are largely defined by the amino acids at two positions, 277 and 279. The N279L mutation reduces the viscosity of β-SkTm to close to β-SmTm values, while both residues contribute to the binding of TnT_1. We also show that removing the first 11 N-terminal amino acids of β-SmTm to make the mutant ΔN-βSmTm results in a 10-fold weakening in actin affinity compared to that of β-SmTm. CD studies show no difference in thermal unfolding between β-SmTm and ΔN-βSmTm; however, the viscosity of ΔN-βSmTm is much lower than that of the control. The results suggest that ΔN-βSmTm was unable to form filaments in solution but can form filaments on actin.

Tropomyosin (Tm)[1] is an α-helical, parallel, two-chain coiled coil which binds along the length of actin filaments in both muscle and non-muscle cells and thus cooperatively regulates the interaction of actin with myosin heads (*1*−*3*). Tropomyosins are expressed in developmental and cell specific patterns. Certain isoforms may be found in more than one cell type or tissue; however, other Tm isoforms are more specific, in particular, those expressed in skeletal and smooth muscle (*4*−*6*).

Tm is expressed via two genes, *Tm1* and *Tm2* (α and β), in fast muscle, and these express high-molecular weight Tm muscle isoforms which are 284 amino acids in length. Isoform diversity (smooth and skeletal) results from the alternative splicing of the two genes (*1*−*3*). The amino-terminal region of muscle tropomyosins is highly conserved (Figure 1). Eight of the first nine amino acids are conserved from *Drosophila* to humans (*7*), and 18 of the first 20 are conserved among all vertebrate muscle tropomyosins. The structure of the N-terminus is crucial for most aspects of tropomyosin function (*8*−*10*), and acetylation of Tm at its N-terminus is essential (*8*−*11*). Bacterially expressed skeletal muscle Tms are not acetylated; therefore, they bind only weakly to actin, but they can regulate binding of S1 to actin in the presence of troponin (*8*). When N-terminal acetylation is mimicked, wild-type binding affinity is restored (*8*). Bacterially expressed β smooth Tm is essentially nonfunctional; however, α smooth Tm is functional but exhibits a 100-fold reduction in actin affinity (*12*). Amino-terminal extensions such as the widely used Ala-Ser form (AS-Tm) have been shown to restore function to near-wild-type behavior for both smooth and skeletal Tms (*9*, *11*, *12*). Skeletal Tm is a mixture of an αα and αβ dimer, whereas smooth Tm is predominantly an αβ dimer (*13*−*18*). Skeletal and smooth Tms encoded by the α-gene differ at exons 2 and 9, while equivalent Tms encoded by the β-gene differ at C-terminal exons 6 and 9 (*2*). Exon 9 is composed of the last 26 amino acids at the C-terminus. The last 20 amino acids at the C-terminus of both skeletal and smooth Tm isoforms are highly conserved among different species; however, there is significant divergence between smooth and skeletal isoforms in this region (Figure 1). α skeletal Tm contains the skeletal specific α exon 9a; similarly, β skeletal Tm expresses the skeletal specific β exon 9a. TnT_1 consists of the tail fragment of troponin T (residues 1−158) which is found in only striated muscle, and exon 9a has been

† This work was supported by National Institutes of Health Grant AR041637.

* To whom correspondence should be addressed: Department of Biosciences, University of Kent, Canterbury CT2 7NY, U.K. E-mail: M.A.Geeves@kent.ac.uk. Tel: 441227827597. Fax: 441227763912.

‡ University of Kent.

§ Boston Biomedical Research Institute.

[1] Abbreviations: Tm, tropomyosin; AS, N-terminal alanine-serine extension; S1, myosin subfragment 1; TnT_1, human cardiac troponin TnT_1 isoform 3; β-SkTm, rat skeletal β-tropomyosin with the AS extension; β-SmTm, chicken gizzard β-tropomyosin with the AS extension; β-SkTm^{CSm}, rat skeletal β-tropomyosin with last 10 amino acids swapped for chicken gizzard β-tropomyosin; ΔN-βSmTm, gizzard β-tropomyosin with an AS extension, with the first 11 N-terminal amino acids truncated.

10.1021/bi701144g CCC: $40.75
Published on Web 12/11/2007

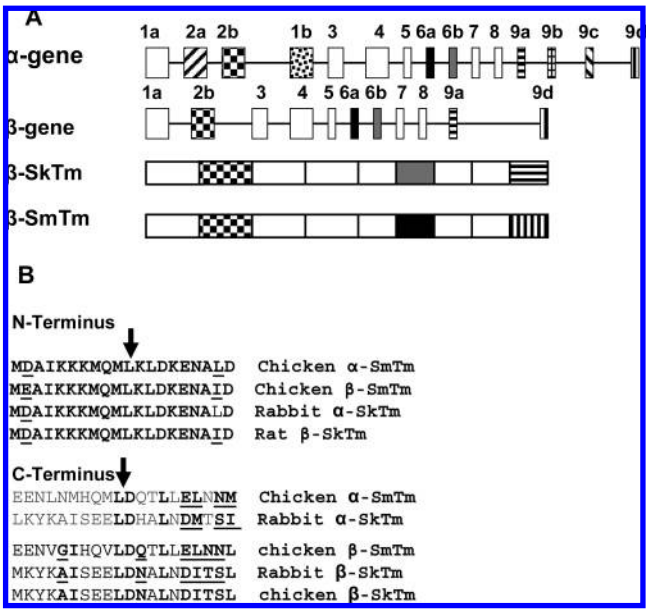

FIGURE 1: (A) Intron−exon organization of the vertebrate α- and β-Tm gene and the associated mRNA products of the β gene adapted from Perry (*3*). The exons are represented by boxes and introns by horizontal lines. The exons are numbered from 1a to 9d to facilitate simple comparison between Tm genes. Both striated and smooth mRNA products contain exon 2a; however, the striated Tm isoform contains exons 6b and 9a, whereas the smooth isoform contains exons 6a and 9d. (B) Sequence alignments of the first and terminal 20 amino acids for α and β smooth and skeletal isoforms. Identical amino acids are in bold, conserved changes underlined, and nonconserved changes in normal text. The figure shows there is a high degree of fidelity between Tm isoforms at the N-terminus, whereas there is a much greater degree of divergence between Tm isoforms at the C-terminus. The truncation of the first 11 amino acids represented by the mutant ΔN-βSmTm is represented by the arrow in the N-terminal amino acid alignments, and the mutation of the last 10 amino acids represented by β-SkTm^{CSm} and α-SkTm^{CSm} is represented by the arrow in the C-terminal amino acid alignments.

implicated in troponin TnT$_1$-dependent regulatory function for both α and β isoforms (*2*, *6*). Smooth α- and β-Tm isoforms contain exon 9d which is common to non-muscle Tm isoforms (*2*); thus, isoform specific function can be attributable to the exon 9-encoded C-terminus (*19*, *20*).

α-Tropomyosins with smooth exon 9d have been shown to bind skeletal muscle actin with an affinity approximately 5 times higher than that of tropomyosins with skeletal exon 9a (*12*, *19*). It has also been demonstrated that the first 18 residues encoded by exon 9a are critical for the interaction of troponin with skeletal α-tropomyosin on the thin filament even in the absence of Ca^{2+} (*20*). In the presence of Ca^{2+}, troponin increases the affinity of α-SkTm for actin at least 50-fold, whereas Tn has little effect on exon 9d-containing α-SmTm (*19*). It has subsequently been proposed therefore that the cooperative activation of actin and Tm containing exon 9d from the closed to the open state by myosin S1 depends on end-to-end interaction (*21*, *22*).

It is well-established that both skeletal and smooth Tm isoforms polymerize in a "head-to-tail" mechanism (*23*, *24*) and that this polymerization is dependent on ionic strength (*21*, *25*) and is important for function in vivo (*26*, *27*). The structure of the N−C overlap had not been fully described until recently due to the low resolution of diffraction of the tropomyosin crystal structure (*28*, *29*). A recent solution NMR study of a fragment of α skeletal Tm has described how the C-terminal residues of the coiled coil splay apart to allow insertion of 11 residues of the N-terminal coiled coil into the resulting cleft (*30*). The plane of the N-terminal coiled coil is rotated 90° relative to the C-terminus (*30*). A consequence of this geometry is that the orientation of postulated periodic actin binding sites on the coiled coil surface is retained from one molecule to the next along the actin filament (*30*, *31*). For αβ-SmTm, there seems to be a specific interaction at the ends which allows the same chain α or β to make equivalent interactions with the same actin subunit along the filament (*32*). The importance of the last 10 amino acids at the C-terminus of Tm and the first 10 amino acids at the N-terminus of Tm is highlighted in the NMR study mentioned above.

In this study, we investigate how the nature of these 10 amino acids at the C-terminus of β-Tm (smooth and skeletal) affects the actin binding and regulatory properties of β-SkTm with the mutant Tm β-SkTm^{CSm}, which was made by swapping the last 10 amino acids of β-SkTm with the corresponding β-SmTm amino acid sequence. We further investigate the importance of specific, nonconserved, residues between β-SkTm and β-SmTm within the last 10 amino acids at the C-terminus using the mutants β-SkTm^{A277T} and β-SkTm^{N279L}, which were made by swapping the β-SkTm residue with the equivalent β-SmTm amino acid.

It has been previously reported that Tm can be cleaved at the N-terminus in vivo between residues 6 and 7 by a proteolytic enzyme transcribed by the *ompT* gene product (*33*). A similar cleavage commonly occurs in *Escherichia coli* expression systems in which a Tm product is produced, which has a mass that corresponds to an 11-amino acid cleavage at the N-terminus. The resulting Tm product (ΔN-βSmTm) can be purified from full-length Tm, and actin binding assays show, surprisingly, that it binds actin, but with a low affinity. This poor affinity for actin is presumably due to the reduction in the number of end-to-end interactions between overlapping Tm species. We therefore investigate the importance of the N-terminus in the formation of the overlap by expressing a Tm with the first 11 amino acids removed from the N-terminus and replacing them with an AS extension. This modified Tm did not bind actin with a high affinity despite the addition of an AS extension.

EXPERIMENTAL PROCEDURES

Construction of Vectors for Expression of Tm. Tm proteins were expressed using the pJC20 vector system as described in ref *34*. pJC20AS.βSkTm^{CSm}, pJC20AS.αSkTm^{CSm}, pJC20AS.βSkA277T, pJC20AS.βSkN279L, and pJC20AS.-βSkA277T/N279L were constructed by cloning *Nde*I- and *Bam*HI-purified, digested PCR-amplified fragments into the *Nde*I and *Bam*HI restriction sites of the pJC20 expression vector. PCR was carried out using pJC20AS.βSk and pJC20AS.αSk vector constructs as the templates. pJC20AS.-βSkTm^{CSm} contains the rat β-SkTm with the last 10 amino acids substituted with the last 10 amino acids of the chicken gizzard β-SmTm, while pJC20AS.αSkTm^{CSm} contains the rabbit α-SkTm with the last 10 amino acids substituted with the last 10 amino acids of the chicken gizzard α-SmTm. pJC20AS.βSk^{A277T}, pJC20AS.βSk^{N279L}, and pJC20AS.-βSk$^{A277T/N279L}$ contain the rat β-SkTm with alanine 277

substituted with threonine, asparagine 279 substituted with leucine, and alanine 277 and asparagine 279 substituted with threonine and leucine, respectively, of the chicken β-SmTm. These express Tm containing an N-terminal Met-Ala-Ser motif (ASTm). The N-terminal Met is removed post-translationally. DNA was sequenced to ensure the fidelity of the PCR amplification. The following nucleotides were used in the PCRs for the construction of pJC20AS.βSkTm^{CSm} and pJC20AS.αSkTm^{CSm}: AS-forward rat β-SkTm, 5′ CC CAT ATG GAC GCC ATC AAG AAG AAG ATG CAG 3′; Rβ-SkTm^{CSm}, 5′ CCG GAT CCT CAG AGG TTG TTC AGC TCC AGC AAG GTC TGG TCC AGC TCC TCG 3′; AS-forward rat α-SkTm, 5′ CC CAT ATG ATG GAC GCC ATC AAG AAG AAG ATG CAG 3′; Rα-SkTm^{CSm}, 5′ CCC GGA TCC TCA CAT GTT GTT TAA CTC CAG TAA AGT TG GTC CAG CTC CTC 3′; Rβ-SkA277T, 5′ CGC GGA TCC TCA GAG GGA AGT GAT GTC ATT GAG GGT GTT GTC 3′; Rβ-SkN279L, 5′ CGC GGA TCC TCA GAG GGA AGT GAT GTC CAG GAG CGC GTT GTC 3′; Rβ-SkA277TN279L, 5′ CGC GGA TCC TCA GAG GGA AGT GAT GTC CAG GAG GGT GTT GTC 3′.

pJC20ΔN.β-SmTm was constructed by cloning *Nde*I- and *Bam*HI-purified, digested PCR-amplified fragments into the *Nde*I and *Bam*HI restriction sites of the pJC20 expression vector. PCR was carried out using the pJC20ASβ-SmTm vector construct as the template. pJC20ΔN.βSmTm contains the chicken β-SmTm with the first 11 amino acids removed and replaced with an AS extension. DNA was sequenced to ensure the fidelity of the PCR amplification as detailed above. The following nucleotides were used in the PCR for the construction of pJC20ΔN.βSmTm: forward ASΔN.βSmTm, 5′ CCC CAT ATG AAA CTG GAC AAG GAG AAC GCC ATC GAC 3′; reverse chk β-Tm, 5′ CGC GGA TCC TCA GAG GTT GTT CAG CTC CAG CAA GGT CTG G 3′.

Plasmid vectors for the expression of chicken gizzard α-SmTm and β-SmTm were constructed as described in ref *35*, and plasmid vectors for the expression of rat skeletal α-SkTm and β-SkTm were constructed as described in ref *36*.

Preparation of Proteins. Recombinant α-SkTm^{CSm}, β-SkTm^{CSm}, A277T, N279L, A277T/N279L, ΔN-βSmTm, α-Tm, and β-Tm were expressed in bacteria (strain BL21 DE3). Cultures (1 L) were grown to exponential phase and induced for 3 h with 100 mg/L IPTG. Cells were harvested and resuspended in 30 mL of cold lysis buffer [20 mM Tris (pH 7.5), 100 mM NaCl, 2 mM EGTA, and 5 mM $MgCl_2$] and lysed by sonication. The majority of *E. coli* proteins were precipitated by being heated to 80 °C for 10 min. The precipitated protein and cell debris were then removed by centrifugation. The soluble Tm was then isoelectrically precipitated at pH 4.5. The precipitate was pelleted and resuspended in 10−20 mL (dependent upon yield) of running buffer [10 mM KP_i (pH 7.0) and 100 mM NaCl] with 10 mg/L DNase and 10 mg/L RNase and incubated at 4 °C for 2 h. The Tm was then further purified using 2 × 5 mL Pharmacia HiTrap-Q columns in tandem and eluted with a 100 to 900 mM NaCl gradient, the Tm eluting at ∼250−350 mM NaCl. Fractions were analyzed by SDS−PAGE, pooled, and concentrated by isoelectric precipitation. Protein concentrations were determined by their absorbance at 280 nm using a molar extinction coefficients (E_{280}) of 16 800 M^{-1} cm^{-1} for α-SkTms, 22 400 M^{-1} cm^{-1} for β-SkTms, and 11 200 M^{-1} cm^{-1} for β-SmTms, for the dimer in 5 mM Tris-HCl buffer (pH 7.0). The molecular masses of all of the expressed Tm proteins were determined using a mass spectrometer with an accuracy of 0.01%. The differences between the obtained values and the expected ones are given in parentheses. The values obtained were 33 010.5 (+1.1) Da for AS.βSm, 32 990.2 (−3.6) Da for AS.β-SkTm, 33 083.9 (0) Da for AS.α-SmTm, 32 838.8 (+0.1) Da for AS.αSk, 33 092.0 (0) Da for β-SkTm^{CSm}, 33 025.1 (+0.3) Da for βSkTm^{A277T}, 32 994.6 (+0.7) Da for βSkTm^{N279L}, and 33 023.9 (0) Da for βSkTm$^{A277T/N279L}$. ΔN-βSmTm was analyzed by mass spectroscopy and N-terminal protein sequencing to confirm the deletion of the first 11 amino acids. ΔN-βSmTm had a mass of 31 681.7 (+2.6) Da as determined by mass spectroscopy which was consistent with the removal of the first 11 amino acids replaced with an AS extension. N-Terminal sequencing data reported ΔN-βSmTm to have an N-terminal sequence of ASKLD, further reinforcing the evidence of this 11-amino acid cleavage.

Human cardiac TnT_1 (TnT_1) was purified as described in refs *37* and *38* from a clone obtained from I. P. Trayer (Birmingham, U.K.). TnT_1 is the N-terminal fragment of troponin T from amino acids 1−158. Briefly, 1 L cultures were grown to exponential phase and induced for 3 h with 100 mg/L IPTG. Cells were harvested and resuspended in lysis buffer [50 mM Tris-HCl (pH 8.0), 1 mM EDTA, 6 M urea, and 1.4 mM β-mercaptoethanol] and lysed by sonication. Cell debris was then removed by centrifugation, and the resulting supernatants were loaded onto an AP Biotech Hi-Trap DEAE Sepharose fast flow column. Proteins were eluted with a gradient of 0 to 600 mM NaCl in lysis buffer. TnT_1-containing fractions were identified via SDS−PAGE. These were pooled and dialyzed against 50 mM sodium acetate (pH 5.0), 1 mM EDTA, 6 M urea, and 1.4 mM β-mercaptoethanol. TnT_1 was then further purified using 2 × 5 mL AP Biotech Hi-Trap CM Sepharose fast flow columns. Proteins were eluted with a gradient of 0 to 600 mM NaCl in lysis buffer, and TnT_1-containing fractions were identified via SDS−PAGE. Urea was removed by dialysis against 50 mM Tris-HCl (pH 8.0), 1 mM EDTA, 1 M KCl, and 1 mM DTT, and the resulting TnT_1 samples were aliquoted and stored at −20 °C. The molar concentration of TnT_1 was determined by bovine serum albumen (BSA) and Bradford assay.

Myosin subfragment 1 (S1) was prepared by chymotryptic digestion of rabbit myosin as described in ref *39*.

Rabbit skeletal actin was purified by the method described in ref *40*. Its molar concentration was determined from its absorbance at 280 nm using an $E^{1\%}$ of 1.104 cm^{-1} and a molecular mass of 42 000 Da. The preparation of pyrene-labeled actin (pyr-actin) was conducted as previously described (*41*). F-Actin was stabilized with phalloidin by incubating a solution of 10 μM pyr-actin with 10 μM phalloidin overnight in 20 mM MOPS, 100 mM KCl, and 5 mM $MgCl_2$ (pH 7.0) at 4 °C.

Cosedimentation and Quantitative Electrophoresis. Cosedimentation assays were performed at 20 °C by mixing 10 μM actin with increasing concentrations of Tm, in the standard experimental buffer [20 mM MOPS, 100 mM KCl, and 5 mM $MgCl_2$ (pH 7.0)], in a total volume of 100 μL. Tm is prespun before use in the cosedimentation assay at

Table 1: Actin Dissociation Constants for β-SkTm^{CSm} and ΔN-βSmTm Compared with Those of β-SkTm and β-SmTm[a]

	$K_{50\%}$ (μM)	h	TnT_1 $K_{50\%}$ (μM)	h	K_T	n
β-SkTm	0.19[b] (±0.04)	1.89[b] (±0.4)	0.09 (±0.03)	2.54 (±1.01)	0.1[b]	7[b]
β-SmTm	0.31[c] (±0.04)	1.33[c] (±0.15)	0.74 (±0.09)	2.07 (±0.47)	0.15[c]	5−9[c]
β-SkTm^{CSm}	0.40 (±0.07)	2.51 (±0.56)	0.85 (±0.07)	2.58 (±0.82)	0.15	5−9
α-SkTm	0.11[d]	2.05[d]	ND[e]	ND[e]	0.1[d]	7[d]
α-SmTm	0.03[c] (±0.005)	2.65[c] (±1.05)	ND[e]	ND[e]	0.1−0.25[c]	5−9[c]
α-SkTm^{CSm}	0.04 (±0.01)	1.49 (±0.35)	ND[e]	ND[e]	ND[e]	ND[e]
ΔN-βSmTm	2.70 (±0.25)	4.57 (±0.39)	ND[e]	ND[e]	0.07−0.12	4−7

[a] $K_{50\%}$ values and the Hill coefficient (*h*) were calculated via the Hill equation from the Tm·actin, TnT_1·Tm·actin binding plots in Figures 2 and 5 and were measured from the best fit to the Hill equation as the free Tm or TnT_1 concentration at which the actin filament is half-saturated by Tm or TnT_1. K_T and *n* values were obtained from the fit of the sigmoidal titration curves to the two-state model of McKillop and Geeves where K_T defines the equilibrium between the closed C-state where only weak myosin binding is possible and the open M-state that allows rigor-like binding and *n* is the cooperative unit size. [KCl] = 100 mM. The values quoted for $K_{50\%}$ are the means and standard deviations of three separate measurements for each protein. [b] Data from ref *51*, [KCl] = 200 mM. [c] Data from ref *12*. [d] Data from ref *52*, [KCl] = 200 mM. [e] Not determined.

Table 2: TnT_1·Actin·Tm Dissociation Constants for the C-Terminal Mutants[a]

	TnT_1 $K_{50\%}$ (μM)	h
β-SkTm	0.1 (±0.09)	2.54 (±1.01)
β-SmTm	0.82 (±0.09)	2.07 (±0.47)
β-SkTm^{A277T}	0.75 (±0.1)	1.3 (±0.16)
β-SkTm^{N279L}	0.63 (±0.08)	1.43 (±0.13)
β-SkTm$^{A277T/N279L}$	1.13 (±0.06)	1.46 (±0.08)

[a] $K_{50\%}$ values and Hill coefficients (*h*) were calculated via the Hill equation from the TnT_1·Tm·actin binding plots in Figure 3 and were measured from the best fit to the Hill equation as the free TnT_1 concentration at which the actin·Tm complex is half-saturated by TnT_1. The values quoted for $K_{50\%}$ are the means and standard deviations of three separate measurements for each protein.

100 000 rpm for 20 min to remove any aggregated protein. The actin was then pelleted along with any bound Tm by ultracentrifugation at 100 000 rpm for 20 min (Beckman Instruments TLA-100.1). Control Tm only sedimentation assays show that ~10% Tm sediments when centrifuged, and this is taken into account when the final Tm binding affinity is calculated. Equivalent samples of pellet and supernatant were then separated by SDS−PAGE. Quantification of proteins was carried out using an Epson Perfection 1640SU scanner with a transparency adaptor attached to a personal computer. Scanned images were analyzed using image-PC (Scion Corp., Frederick, MD). The fraction of Tm bound to actin (fractional saturation) was estimated from the ratio of the density of the actin and Tm bands in the pellet gel and plotted against the free Tm concentration where a fractional saturation value of 1 for a fully saturated actin filament corresponds to a binding stoichiometry of seven actins for each Tm bound. The $K_{50\%}$ values were determined after fitting the curves with the Hill equation (eq 1), and the values are given in Table 1.

$$\theta = \frac{[\mathrm{Tm}]^h}{K_{50\%}{}^h + [\mathrm{Tm}]^h} \quad (1)$$

where *h* is the Hill coefficient, θ is the fractional saturation of actin with Tm, and $K_{50\%}$ is the Tm concentration required for 50% saturation of actin. The measurements are routinely done three times for each protein, and the errors in Tables 1 and 2 reflect the standard deviation observed for the three separate measurements.

Cosedimentation and Quantitative Electrophoresis with TnT1. Cosedimentation assays with TnT_1 were performed at 20 °C in the standard experimental buffer as described above by mixing 10 μM actin with 2 μM Tm and increasing concentrations of TnT_1. Quantification and analysis of proteins were carried out as described above.

Cosedimentation and Quantitative Electrophoresis with S1. Cosedimentation assays with S1 were performed at 20 °C in the standard experimental buffer as described above by mixing 10 μM actin with 10 μM S1 and increasing concentrations of Tm. Quantification and analysis of proteins were carried out as described above.

Fluorescence Titrations. Fluorescence titrations were measured at 20 °C using a Perkin-Elmer Life Sciences 50B spectrofluorimeter with excitation at 365 nm with a 10 nm bandwidth and measuring emission at 405 nm with a 15 nm bandwidth. A total working volume of 2 mL of 50 nM phalloidin-stabilized pyrene-labeled actin, 2 μM Tm in 20 mM MOPS (pH 7.0), 100 mM KCl, and 5 mM $MgCl_2$ was used in a 10 mm × 10 mm cell being stirred constantly using a magnetic stirrer below the light path of the instrument. Autotitrations were conducted by the continuous addition of a 5 μM S1 stock solution at a rate of 12 μL/min, using a Harvard Apparatus Syringe Infusion Pump 22, driving a 100 μL glass syringe (Hamilton). Data were acquired over a period of 250 s, with data points being collected every 0.5 s, using an integration time of 0.45 s. Buffer solutions for the titrations were as previously described and were filtered using a 0.22 μm disposable syringe filter to remove dust particles that may produce significant noise in the stirred cell at the low levels of sample fluorescence used.

The equilibrium binding of myosin S1 to actin is normally observed as a hyperbolic binding curve as expected for an interaction between two independent molecules. When tropomyosin is present, the binding becomes sigmoidal which is indicative of a cooperative binding process. The cooperative binding curves from the titrations were fitted using a two-state version of the McKillop and Geeves model with a varying cooperative unit size (*36*, *42*). In this model, the actin·Tm filament can be in one of two states, closed or open [currently interpreted as the Tm sitting in different positions on the actin filament surface (*43*)]. In the closed state, the Tm can inhibit myosin binding. In the open state, myosin can bind freely. The binding of a single myosin head to an actin·Tm filament requires Tm to move to a non-inhibitory position. In doing so, the Tm exposes other actin sites to allow free binding of myosin. Hence, the system appears cooperative. The average number of actin sites that become relieved of inhibition when one myosin binds is called the

apparent cooperative unit size. The binding isotherm can be described by eq 2

$$\theta = \frac{K_1[\mathrm{M}]K_\mathrm{T}[(1 + K_2)P^{n-1} + Q^{n-1}]}{K_\mathrm{T}P^n + Q^n} \quad (2)$$

$$\theta = \frac{F_0 - F}{F_0 - F_\infty} \quad (3)$$

where θ represents the fraction of total actin sites occupied, K_1 represents the weak S1 binding, [M] is the concentration of free S1 heads, n is the cooperative unit size, $P = 1 + K_1[\mathrm{M}](1 + K_2)$, and $Q = 1 + K_1[\mathrm{M}]$. K_T defines the equilibrium between the closed C-state where only weak myosin binding is possible and the open M-state that allows rigor-like binding. The fluoresence signal (F) is related to θ through eq 3, in which F_0 is the initial fluorescence before addition of S1 and F_∞ is the fluorescence at saturation with S1.

Viscosity. Protein samples (20 μM) were run through a Cannon-Manning semi-microviscometer (C150) in a volume of 1 mL at 24 ± 1 °C in 2 mM MOPS (pH 7.0) and 5 mM $MgCl_2$ with the KCl concentration increasing from 0 to 500 mM. Kinematic viscosity was calculated for each sample from the kinematic viscosity constant of the viscometer and the average efflux time, which was calculated using five observations for each sample.

Circular Dichroism. Circular dichroism studies of β-proteins were performed using a Jasco 715 spectropolarimeter. Thermal data were obtained automatically as ellipticity values of 222 nm at a scan speen of 1 deg/min. The sample was measured in a 1 mm cuvette.

RESULTS

Preparations of bacterially expressed β-SmTm constructs showed the presence of a cleaved product of β-SmTm which had a weak binding affinity for actin. A sample of the naturally cleaved β-SmTm was analyzed by mass spectroscopy and was found to have a mass of 31 522.5 Da, a mass consistent with the deletion of the first 11 amino acids. N-Terminal sequencing produced a sequence of KLDKE, which was consistent with the sequence from the 12th amino acid. We therefore expressed the identical fragment and used this in the following studies.

Affinity of Tropomyosin for Actin. The affinity of Tm constructs for actin was measured and compared to that of native Tm using a cosedimentation assay. An example of an SDS−PAGE gel used for determining binding affinities is illustrated in Figure 2A. The two gels show an experiment involving β-SmTm. The top gel shows the pellets and the bottom gel the supernatants from the cosedimentation assay. Each sample contained 10 μM actin incubated with increasing concentrations of Tm from 0.1 μM (lane 1) to 8 μM (lane 10). In both gels, actin is the upper band and the density of this band remains practically constant in all the samples, with the majority of the actin appearing in the pellet as expected (lanes 1−10). The lower band on both gels is Tm, and the optical density of the Tm band increases from the lowest-Tm concentration sample (lane 1) to the highest-Tm concentration sample (lane 10). The fraction of Tm bound to actin (fractional saturation) was estimated from the ratio

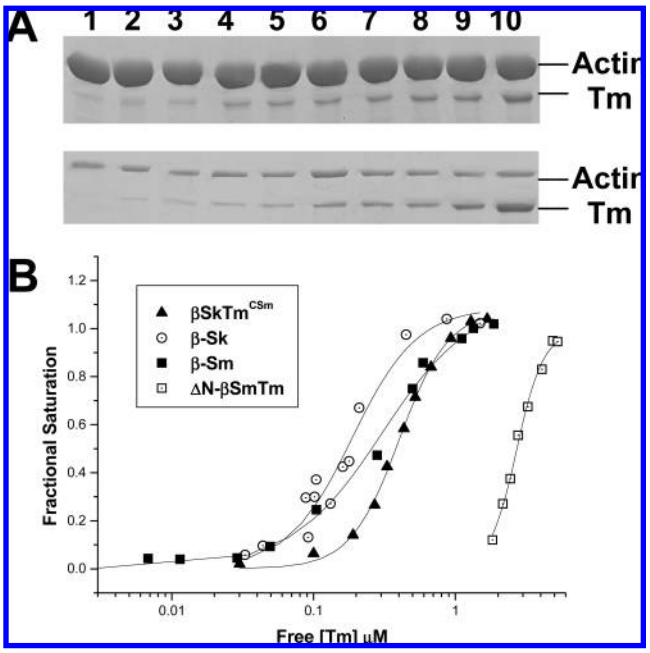

FIGURE 2: (A) Sedimentation assay of tropomyosin binding to actin. Actin (10 μM) and β-SmTm (0.1−4 μM) were spun at 100000*g*, and the pellets and supernatants were analyzed by SDS−PAGE. The fraction of β-SmTm, bound to actin, was calculated from the relative band densities. (B) Analysis of the fraction of β-SkTm (○), β-SmTm (■), β-SkTm^{CSm} (▲), and ΔN-βSmTm (□) binding to actin from the relative band densities. Binding constants ($K_{50\%}$), the fraction of Tm bound to actin, were estimated from the density of the bands in the pellet and plotted against the free Tm concentration. The fitted line is the least-squares best fit to the Hill equation. Conditions: 100 mM KCl, 5 mM $MgCl_2$, 20 mM MOPS (pH 7.0), 20 °C.

of the density of the actin and Tm bands in the pellet gel and plotted versus the free Tm concentration (Figure 2B).

β-SkTm^{CSm} bound actin with an affinity similar to that of β-SmTm which was ∼1.5−2-fold weaker than that of β-SkTm ($K_{50\%}$ = 0.4, 0.31, and 0.19 μM, respectively). α-SkTm^{CSm} bound actin with an affinity similar to that of α-SmTm which was ∼3-fold tighter than that of α-SkTm ($K_{50\%}$ = 40, 35, and 100 nM, respectively), thus suggesting that this 10-amino acid C-terminal region of Tm is important in determining the affinity for actin.

ΔN-βSmTm surprisingly bound actin with a reasonable affinity which was ∼10-fold weaker than that of the β-SmTm control ($K_{50\%}$ = 2.7 and 0.3 μM, respectively). In the presence of S1 in a 1:1 ratio with actin, the affinity of ΔN-βSmTm increases by ∼10-fold ($K_{50\%}$ = 70 nM), suggesting in agreement with refs *44* and *48* that S1 enhances the binding of SmTm to actin. The increase in actin affinity in the presence of S1 is accompanied by a reduction in cooperativity, ΔN-βSmTm (h = 4.57) and S1 (h = 3.5).

Thermal Stability. Since removal of the first 11 amino acids could alter the stability of the protein, we examined the melting profiles of ΔN-βSmTm and β-SmTm as shown in Figure 3A. ΔN-βSmTm unfolds with a profile which is very similar to that of β-SmTm. The major transition at 42 °C appears identical with a slight loss of stability on the region before the major transition (25−35 °C). This shows that removing the first 11 amino acids of β-SmTm does not significantly alter its thermal stability. Figure 3B shows that β-SkTm melts at a temperature ∼7 °C lower than that of

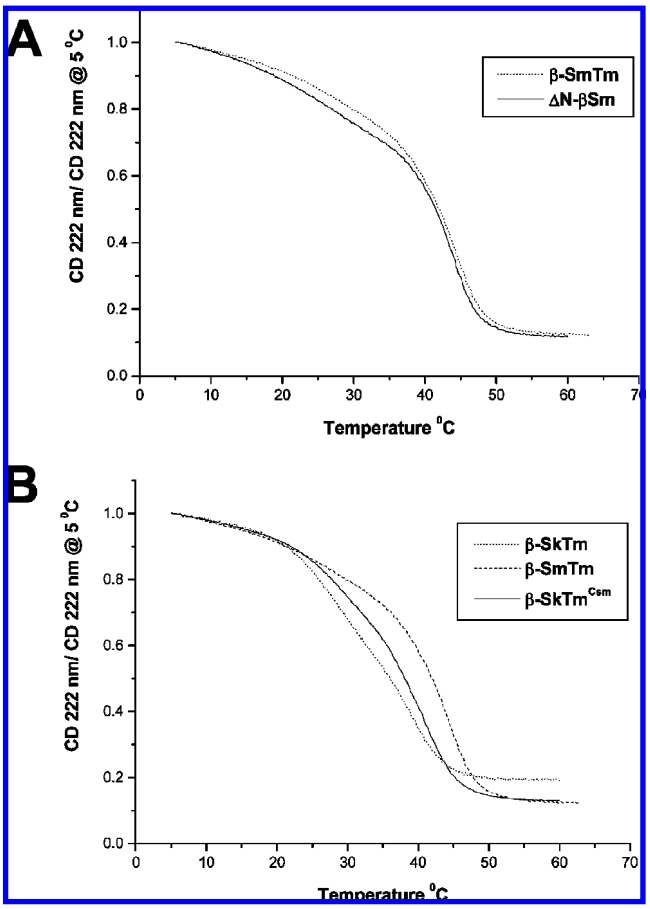

FIGURE 3: (A) Comparison of the thermal unfolding of Tm constructs. The relative α-helical content is calculated from the molar ellipticity at 222 nm of Tm at a particular temperature relative to that of Tm at 5 °C. Conditions: 20 mM KPO_4 (pH 7.0), 500 mM NaCl, 1 mM DTT, 5 mM $MgCl_2$.

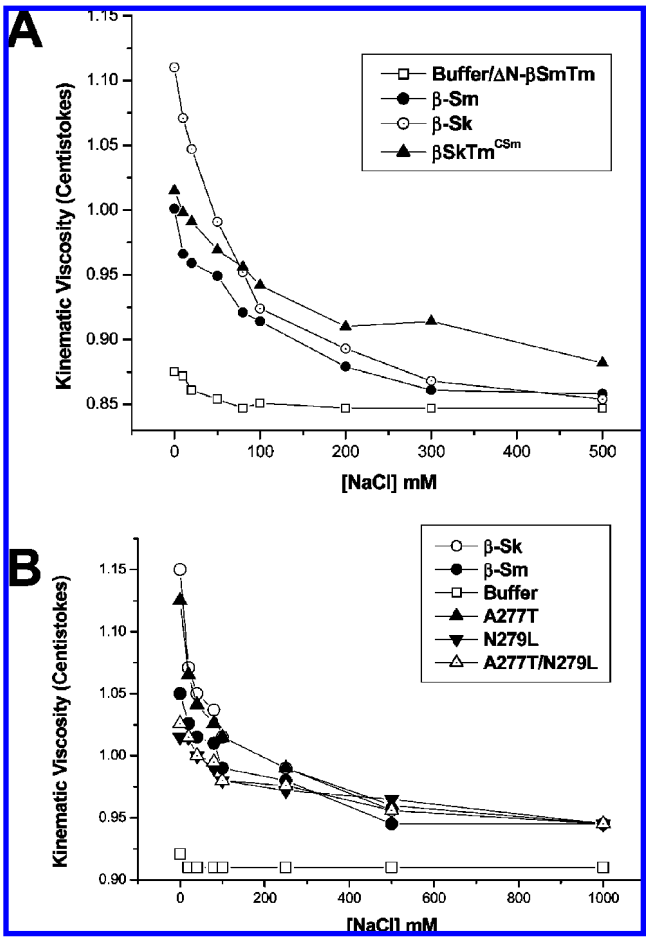

FIGURE 4: Salt dependence of the specific viscosity for (A) β-SmTm (●), β-SkTm (○), β-SkTm^{CSm} (▲), and buffer with ΔN-βSmTm (□) and (B) β-SmTm (●), β-SkTm (○), A277T (▲), N279L (▼), and A277T/N279L (△) compared to the buffer (□). Conditions: 20 μM Tm in 2 mM MOPS (pH 7.0), 5 mM $MgCl_2$, 24 °C.

β-SmTm. β-SkTm^{CSm} is slightly more stable than β-SkTm, but it still melts at a temperature ~4.5 °C lower than that of β-SmTm.

End-to-End Interactions. Previous studies have indicated that specific viscosity is a measure of Tm end-to-end polymerization at low salt concentrations (*21*, *24*, *45*, *46*). Viscosity measurements were taken using each of the Tms at 20 μM at increasing salt concentrations (Figure 4A). The viscosity of β-SkTm^{CSm} and ΔN-βSmTm was compared to that of β-SkTm and β-SmTm. It can be seen from the graph in Figure 4A that at low salt concentrations β-SkTm had the greatest viscosity and the viscosity of β-SmTm was much lower. β-SkTm^{CSm} exhibited a viscosity which was slightly higher than that of β-SmTm but was much more similar to that of β-SmTm than it was to that of β-SkTm, and this result indicates an important role for the C-terminal 10 amino acids in the end-to-end interactions between tropomyosin molecules. The viscosity of ΔN-βSmTm was indistinguishable from that of the buffer, and this result observed for ΔN-βSmTm is consistent with ΔN-βSmTm's inability to form Tm filaments in solution in the absence of actin.

Affinity of TnT_1 for C-Terminal Tropomyosin Mutants. The affinity of TnT_1 for β-SkTm^{CSm} bound to actin was measured and compared to those of β-SkTm and β-SmTm by cosedimentation assay as shown in Figure 5. The fraction of TnT_1 bound to actin·Tm (fractional saturation) was estimated from the ratio of the density of the actin·Tm and TnT_1 bands in the pellet gel (Figure 5A) and plotted against the free TnT_1 concentration (Figure 5C). Figure 5B shows that 12% TnT_1 sediments when centrifuged either by itself or in the presence of actin, and the calculated $K_{50\%}$ values account for this. The $K_{50\%}$ values were determined after fitting the curves with the Hill equation (eq 1), and the values are given in Table 1.

TnT_1 bound the actin·β-SkTm^{CSm} complex with an affinity similar to that of β-SmTm which was ~10-fold weaker than that of β-SkTm ($K_{50\%}$ = 0.85 μM, 0.74 μM, and 90 nM, respectively), in agreement with previous studies on α-Tm (*19*, *20*). The results therefore confirm that exon 9 is important for Tm−TnT_1 binding in both α- and β-Tm and suggests that binding of TnT_1 to Tm is dominated by the last 10 amino acids of Tm.

Regulation of Binding of S1 to Pyr-Actin. The interaction between actin and myosin subfragment 1 (S1) in vertebrate striated muscle is regulated by the thin filament proteins tropomyosin (Tm) and troponin (Tn). The steric blocking model is the most commonly quoted molecular interpretation of this regulation mechanism in which tropomyosin, in the absence of calcium, physically blocks the myosin binding site on actin. Binding of calcium to troponin causes a conformational change in the thin filament which results in

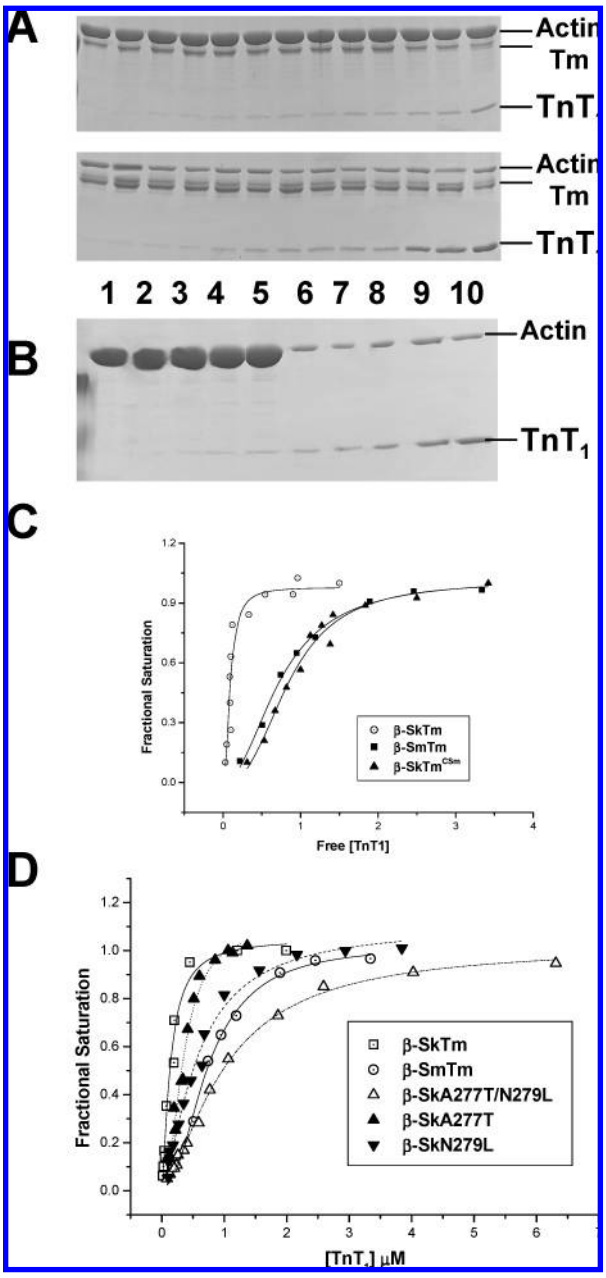

FIGURE 5: Sedimentation assay of binding of TnT_1 to actin·β-Tm isoforms. (A) Actin (10 μM), β-SkTm^{A277T} (2 μM), and increasing TnT_1 concentrations (0.05−4 μM) were spun at 100000*g* and the supernatants analyzed by SDS−PAGE. The fraction of TnT_1 bound to actin·β-Tm was calculated from the relative band densities. (B) Control sedimentation assay of TnT_1 with 10 μM actin. Lanes 1−5 contained the pellet fractions and lanes 6−10 the supernatant fractions. TnT_1 was added at concentrations of 0.4, 0.8, 1, 2, and 4 μM to each of the samples in lanes 1−5 and 6−10, respectively. (C) Analysis of the fraction of TnT_1 binding to actin·β-SkTm and β-SmTm·β-SkTm^{CSm} and (D) actin-A277T/N279L, A277T, and N279L from the relative band densities. Binding constants ($K_{50\%}$), the fraction of TnT_1 bound to actin·Tm, were estimated from the density of the bands in the pellet and plotted against the free TnT_1 concentration. The fitted line is the least-squares best fit to the Hill equation. Conditions as described above.

tropomyosin moving over the surface of actin to a nonblocking position (*42*).

Equilibrium titrations of pyrene-labeled actin with S1 were conducted to assess whether expressed β-SkTm^{CSm} and ΔN-βSmTm regulated the binding of S1 to actin compared to β-SkTm and β-SmTm. Panels A and B of Figure 6 show

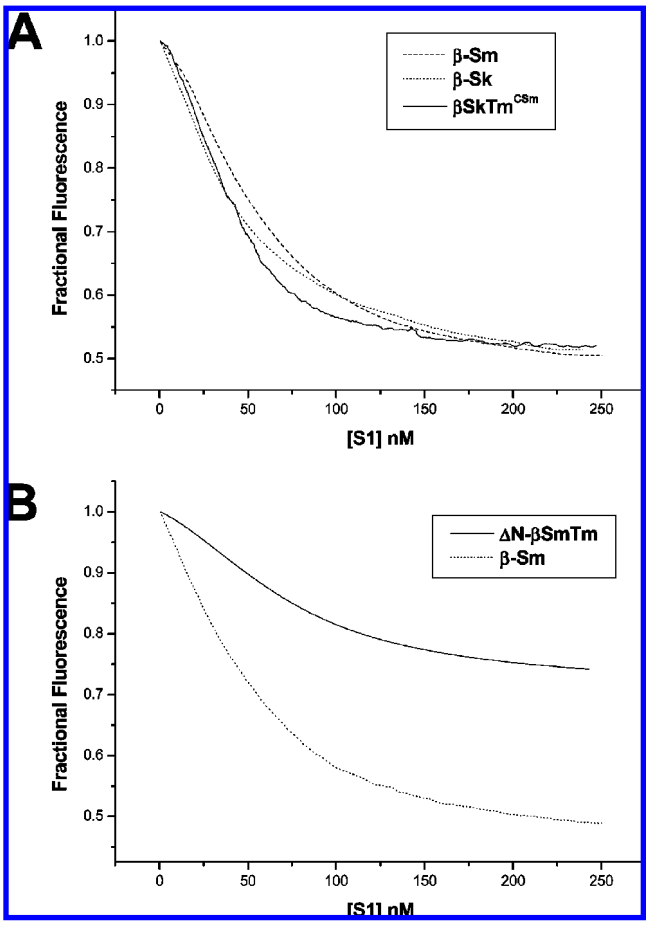

FIGURE 6: Fluorescence titration of pyr-actin by S1 in 50 nM pyr-actin with (A) 2 μM β-SkTm (···), β-SmTm (- - -), and β-SkTm^{CSm} (—) or (B) 5 μM ΔN-βSmTm (—) and β-SmTm (- - -) with an S1 concentration between 0 and 250 nM. The data were fitted to the two-state cooperative binding model. Fitted parameters are given in Table 1. Conditions as described above.

the raw titration curves in which 5 μM S1 is continuously titrated into a cuvette containing 50 nM phalloidin-stabilized pyr-actin, saturated with Tm (2 μM for β-SkTm, β-SmTm, or β-SkTm^{CSm} and 5 μM for ΔN-βSmTm). The sigmoidal shapes of the curves show that Tm regulates binding of S1 to actin. These curves were fitted to a two-state version of the Mckillop and Geeves model (*42*). The value of K_1 (the weak binding) was seen to be $\sim 1.8 \times 10^5$ s^{-1} M^{-1} for all the reconstituted filaments. The shape of the curves is therefore defined by the value of K_T ([M]−[C] equilibrium), and n (the apparent cooperative unit size). Note that as reported previously the values of K_T and n are not independent; equivalent fits indistinguishable from the data can be obtained with a range of n and K_T values which are indicated in Table 1. Larger values of n require smaller values of K_T. Table 1 shows the K_T values that were measured for each Tm after fitting to the two-state model.

β-SkTm^{CSm} regulated binding of S1 to actin ($K_T = 0.15$, and $n = 5-9$) in a way similar to those of both β-SkTm and β-SmTm ($K_T = 0.1$, and $n = 7$; $K_T = 0.15$, and $n = 5-9$). The K_T and n values for β-SkTm^{CSm} show that the mutation has not unduly affected the ability of the tropomyosin to regulate S1 binding. No significant role could be assigned to the C-terminus in regulating binding of S1 to actin using this assay, as the K_T and n values are similar for both β-SkTm and β-SmTm at the level of sensitivity of the

assay. ΔN-βSmTm also regulated binding of S1 to actin as shown by the sigmoidal nature of the curve (Figure 6B) with similar values of K_T and n ($K_T = 0.07-0.12$, and $n = 4-12$). The curve representing ΔN-βSmTm exhibited a smaller decrease in fluorescence compared to the β-SmTm control, a result which we cannot fully explain at this time.

TnT_1 Binding and End-to-End Interactions of β-SkTm C-Terminal Point Mutations. The affinity of TnT_1 for A277T, N279L, and A277T/N279L was measured and compared to those of β-SkTm and β-SmTm by a cosedimentation assay as described above (Figure 5). The $K_{50\%}$ values were determined after fitting the curves with the Hill equation (eq 1), and the values are given in Table 2. TnT_1 bound the three C-terminal mutants (i.e., A277T, N279L, and A277T/N279L) with an affinity similar to that of β-SmTm ($K_{50\%} = 0.75$, 0.63, and 1.13 μM, respectively). These results suggest that the amino acids at positions 277 and 279 are involved in Tm−TnT_1 interactions, with alanine 277 being possibly more important than the asparagine at position 279.

Figure 4B shows the viscosity of the three C-terminal mutants compared to those of β-SkTm and β-SmTm. At low salt concentrations, N279L and A277T/N279L exhibited a lower viscosity than β-SkTm, a viscosity similar to that of β-SmTm. A277T, however, exhibited a viscosity much more similar to that of β-SkTm than that of β-SmTm at low salt concentrations. These results thus suggest that the asparagine at position 279 of β-SkTm is important in the end-to-end interactions between adjacent Tm molecules. The alanine at position 277, however, does not seem to be significantly involved in these interactions.

DISCUSSION

To investigate the role of the N-terminus in the formation of the overlap region between neighboring Tms, we have expressed a shorter β-SmTm (ΔN-βSmTm) with truncation at amino acid 11. The N-terminus is highly conserved between α- and β-Tms (*7*), and previous studies have shown that acetylation of the amino terminus is essential for Tm function (*8*, *9*, *27*, *47*). ΔN-βSmTm exhibits thermal unfolding properties which are not significantly different from those of the parent protein. Regulation of binding of S1 to actin·Tm is also largely unaffected by the deletion; however, the viscosity of this mutant is virtually indistinguishable from that of the buffer in contrast to the intact parent protein. The extent of actin binding is also reduced by ∼10-fold, but the binding remains highly cooperative as shown by the large Hill coefficient. A Tm without strong end-to-end interactions might be expected to bind in a way that results in a "parking problem" as tropomyosin binds actin such that the filament stoichiometry could not adhere to the 7:1 actin:Tm ratio. Although the actin affinity of ΔN-βSmTm is weak, the data seems to suggest that this Tm, once bound to actin, can form continuous strands on the actin surface. In the presence of S1, the affinity of Tm for actin is increased by ∼10-fold, resulting in an actin affinity which is similar to that of β-SmTm. The S1-induced increase in affinity for Tm·actin has been observed for many Tm isoforms and has been interpreted as being due to a direct interaction between S1 and Tm (*44*), or due to an S1-induced change in actin conformation (*48*). The S1-induced increase in the affinity of Tm for actin seen here is accompanied by a small decrease in cooperativity. This agrees well with previously published data (*48*), where a method more sensitive than our assay was used to show that the cooperativity of Tm·actin binding was reduced by approximately 5-fold in the presence of S1 (*44*). The low viscosity and weak actin binding data for ΔN-βSmTm are consistent with an initiation−polymerization model of Tm binding to actin (*49*) where the end-to-end interactions play a major role in defining the polymerization of Tm on actin.

A curious aspect of this deletion mutant is how well it binds to actin despite the deletion of 1.5 heptads from the end of the Tm and the effective shortening of the Tm by ∼25% of an actin binding domain (∼42 amino acids) (*23*). It would not be expected that Tm could form a coherent thread along the actin surface with such a mismatch of periodicity unless the binding between actin and specific sites on Tm is not as rigorous as currently defined.

We also investigated the role of the C-terminus in the formation of the overlap region using the β isoforms. It has been shown previously that for the α muscle Tm isoforms, the C-terminus is extremely important in defining the different properties (e.g., actin binding affinity, cooperativity, troponin binding) of smooth and skeletal isoforms (*9*, *19*, *22*, *50*). These can be ascribed to exon 9 which is the last 26 amino acids of Tm (*19*), and further studies have shown the importance of residues 276 and 277 for the actin binding affinity of unacetylated α isoforms (*50*). The skeletal α isoform expresses exon 9a, and it is this exon that gives skeletal isoforms their ability to bind TnT (*9*, *20*). The entire exon 9a is required for TnT to promote high-affinity binding to actin, and the first 18 residues encoded by exon 9a are critical for the interaction of TnT with Tm on the thin filament even in the absence of Ca^{2+} (*20*). The N- and C-termini of the skeletal isoform therefore regulate myosin S1 binding by forming a ternary complex with TnT. The highly cooperative activation of actin by Tm isoforms expressing exon 9d, from the closed to the open state by myosin S1, however, depends on end-to-end interaction (*21*, *22*).

We have now confirmed the importance of the last 10 amino acids in β-Tm which are now known to be involved in the overlap complex (*30*) in defining the properties of smooth and skeletal Tm isoforms. We have further identified important roles for the amino acids present at positions 277 and 279. We show using domain swap and point mutations that actin binding and the regulation of binding of S1 to actin are not significantly changed; however, viscosity and TnT_1 binding are significantly altered, and these are properties which are directly associated with the overlap region.

The residues at positions 277−279 are highly conserved in vertebrate skeletal α- and β-Tms, and this suggests that they are important in end-to-end complex formation and troponin T interactions. Our data show that exchanging A277 and N279 of β-SkTm for residues T277 and L279 in β-SmTm dramatically alters the affinity of troponin T for the actin·Tm complex. In contrast, only the N279L mutant reduces the viscosity of β-SkTm back to β-SmTm values. These two observations suggest that the amino acid at position 279 is involved in the stabilization of the overlap complex, whereas both of the amino acids at positions 277 and 279 are involved in binding troponin T. This interpretation is consistent with recently published structural data on the overlap complex (*30*).

The NMR study of the overlap complex formed by leucine zipper-stabilized N- and C-terminal fragments of α skeletal tropomyosin has shown that the chains of the C-terminal coiled coil splay apart to allow insertion of the last 11 amino acids of the N-terminal coiled coil into the resulting cleft (*30*). The overlap complex is stabilized by hydrophobic interactions between the *a* and *d* positions of the N-terminal domain's coiled coil and residues of the C-terminal domain. Interchain interactions are mostly hydrophobic in α-Tm, and A277 is involved in the formation of a hydrophobic intermolecular interface as well as a specific interaction with the side chains of K5. Ionic interactions are also apparent in stabilizing the overlap complex. D275 forms an intrachain ionic interaction with N279; therefore, a change to leucine at this amino acid position could lead to a local destabilization in the Tm chain which could reduce the strength of end-to-end interaction relative to that of *β*-SkTm. This may therefore account for the reduction in the viscosity of both the *β*-SmTm isoform and the mutant proteins N279L and A277T/N279L.

Upon formation of an end-to-end complex, there is a significant change in the ^{13}C chemical shift displacement of A277, and this change reflects an alteration in hydrophobic packing. Measurements of the R_2 relaxation rates of the amide backbone for C-terminal residues upon complex formation show that L278 along with Q263 exhibits a 2-fold higher value than the other residues, indicating that this residue exchanges between multiple conformations on complex formation. Residues Q263 and L278 are both part of the troponin T−Tm interface, suggesting that the conformational dynamics present in the overlap complex may contribute to the formation of the ternary complex with troponin T. This structural information is consistent with position 279 being important in the overlap complex, and both positions 277 and 279 being important in the formation of a ternary complex with TnT. Swapping the residues at positions 277 and 279 in *β*-Sk for the corresponding residues of *β*-SmTm could therefore facilitate deleterious changes in the conformational dynamics within the overlap complex at the important residue 278 which results in this reduction in TnT_1 affinity, which is representative of the *β*-SmTm isoform.

In summary, we have demonstrated the essential role of the 10−11 N- and C-terminal residues of *β*-Tm in forming head-to-tail filaments and in binding TnT_1. The smooth and skeletal *β* isoforms differ in these properties yet are identical at the N-terminus and have only nonconserved sequence changes at two sites where A277 and N279 are replaced by T277 and L279, respectively, in *β*-SmTm. Both residues contribute to the difference in TnT_1 binding, while the ability to form viscous filaments is largely defined by the side chain at position 279.

ACKNOWLEDGMENT

We thank Nancy Adamek for technical assistance in the production of actin and S1 proteins used in this study, Dr. Ian Trayer for the provision of the TnT_1 clones, Amy Hopping for assistance with circular dichroism measurements with the ΔN-*β*SmTm and *β*-Sm proteins, and Dr. Steve Martin at NIMR, Mill Hill, for further help with circular dichroism measurements with the *β*-$SkTm^{Csm}$ mutant.

REFERENCES

1. Smillie, L. B. (1979) Structure and functions of tropomyosins from muscle and non-muscle sources, *Trends Biochem. Sci. 4*, 151−154.
2. Lees-Miller, J. P., and Helfman, D. M. (1991) The molecular basis for tropomyosin diversity, *BioEssays 13*, 429−437.
3. Perry, S. V. (2001) Vertebrate tropomyosin: Distribution, properties and function, *J. Muscle Res. Cell Motil. 22*, 5−49.
4. Ruiz-Opazo, N., and Nadal-Ginard, B. (1987) Alpha tropomyosin gene organisation. Alternative splicing of duplicated isotype-specific exons accounts for the production of smooth and striated muscle isoforms, *J. Biol. Chem. 262*, 4755−4765.
5. Lees-Miller, J. P., Goodwin, L. O., and Helfman, D. M. (1990) Three novel brain isoforms are expressed from the rat α-tropomyosin gene through the use of alternative promoters and alternative RNA processing, *Mol. Cell. Biol. 10*, 1729−1742.
6. Wieczorek, D. F., Smith, C. W. J., and Nadal-Ginard, B. (1988) The rat α-tropomyosin gene generates a minimum of six different mRNA's coding for striated, smooth, and non-muscle isoforms by alternative splicing, *Mol. Cell. Biol. 8*, 679−694.
7. Basi, G. S., and Storti, R. V. (1986) Structure and DNA sequence of the Tm1 gene from *Drosophila melanogaster*, *J. Biol. Chem. 261*, 817−827.
8. Heald, R. W., and Hitchcock-Degregori, S. E. (1988) The structure of the amino terminus of tropomyosin is critical for binding to actin in the absence and presence of troponin, *J. Biol. Chem. 263*, 5254−5259.
9. Palm, T., Greenfield, N. J., and Hitchcock-Degregori, S. E. (2003) Tropomyosin ends determine the stability and functionality of overlap and troponin T complexes, *Biophys. J. 84*, 3181−3189.
10. Kluwe, L., Maeda, K., Miegel, A., Fujita-Becker, S., Maeda, Y., Talbo, G., Houthaeve, T., and Kellner, R. (1995) Rabbit skeletal muscle αα-tropomyosin expressed in baculovirus-infected insect cells possesses the authentic N-terminus structure and functions, *J. Muscle Res. Cell Motil. 16*, 103−110.
11. Monteiro, P. B., Lataro, R. C., Ferro, J. A., and Reinach, F d. C. (1994) Functional α-tropomyosin produced in *Escherichia coli*. A dipeptide extension can substitute the amino-terminal acetyl group, *J. Biol. Chem. 269*, 10461−10466.
12. Coulton, A., Lehrer, S. S., and Geeves, M. A. (2006) Functional homodimers and heterodimers of recombinant smooth mucle tropomyosin, *Biochemistry 45*, 12853−12858.
13. Eisenberg, E., and Kielley, W. W. (1974) Troponin-tropomyosin complex. Column chromatographic separation and activity of the three active troponin components with and without tropomyosin present, *J. Biol. Chem. 249*, 4742−4748.
14. Lehrer, S. S. (1975) Intramolecular crosslinking of tropomyosin via disulfide bond formation: Evidence for chain register, *Proc. Natl. Acad. Sci. U.S.A. 72*, 3377−3381.
15. Bronson, D. D., and Schachat, F. H. (1982) Heterogeneity of contractile proteins. Differences in tropomyosin in fast, mixed, and slow skeletal muscles of the rabbit, *J. Biol. Chem. 257*, 3937−3944.
16. Sanders, C., Burtnik, L. D., and Smillie, L. B. (1986) Native chicken gizzard tropomyosin is predominantly a *βγ*-heterodimer, *J. Biol. Chem. 261*, 12774−12778.
17. Jancso, A., and Graceffa, P. (1990) Smooth muscle tropomyosin coiled-coil dimers. Subunit composition, assembly and end-to-end interaction, *J. Biol. Chem. 266*, 5891−5897.
18. Lehrer, S. S., and Stafford, W. F. (1991) Preferential assembly of the tropomyosin heterodimer: Equilibrium studies, *Biochemistry 30*, 5682−5688.
19. Cho, Y. J., and Hitchcock-Degregori, S. E. (1991) Relationship between alternatively spliced exons and functional domains in tropomyosin, *Proc. Natl. Acad. Sci. U.S.A. 88*, 10153−10157.
20. Hammell, R. L., and Hitchcock-Degregori, S. E. (1996) Mapping the functional domains within the carboxyl terminus of α-tropomyosin encoded by the alternatively spliced ninth exon, *J. Biol. Chem. 271*, 4236−4242.
21. Lehrer, S. S., Golitsina, N. L., and Geeves, M. A. (1997) Actin-tropomyosin activation of myosin subfragment 1 ATPase and thin filament cooperativity. The role of tropomyosin flexibility and end-to-end interactions, *Biochemistry 36*, 13449−13454.
22. Moraczewska, J., and Hitchcock-Degregori, S. E. (2000) Independent functions for the N- and C-termini in the overlap region of tropomyosin, *Biochemistry 39*, 6891−6897.

23. McLachlan, A. D., and Stewart, M. (1975) Tropomyosin coiled-coil interactions: Evidence for an unstaggered structure, *J. Mol. Biol. 98*, 293−304.
24. Ooi, T., Mihashi, K., and Kobayashi, H. (1962) On polymerisation of tropomyosin, *Arch. Biochem. Biophys. 98*, 1−11.
25. Sousa, A. D., and Farah, C. S. (2002) Quantitative analysis of tropomyosin linear polymerization equilibrium as a function of ionic strength, *J. Biol. Chem. 277*, 2081−2088.
26. Johnson, P., and Smilie, L. B. (1977) Polymerisability of rabbit skeletal tropomyosin: Effects of enzymic and chemical modifications, *Biochemistry 16*, 2264−2269.
27. Hitchcock-Degregori, S. E., and Heald, R. W. (1987) Altered actin and troponin binding of amino-terminal variants of chicken striated muscle α-tropomyosin expressed in *Escherichia coli*, *J. Biol. Chem. 262*, 9730−9735.
28. Phillips, G. N., Jr., Fillers, J. P., and Cohen, C. (1986) Tropomyosin crystal structure and regulation, *J. Mol. Biol. 192*, 111−131.
29. Whitby, F. G., and Phillips, G. N., Jr. (2000) Crystal structure of tropomyosin at 7 Å resolution, *Proteins 38*, 49−59.
30. Greenfield, N. J., Huang, Y. J., Swapna, G. V. T., Bhattacharya, A., Rapp, B., Singh, A., Montelione, G. T., and Hitchcock-Degregori, S. E. (2006) Solution NMR structure of the junction between tropomyosin molecules: Implications for actin binding and regulation, *J. Mol. Biol. 364*, 80−96.
31. Greenfield, N. J., Swapna, G. V., Huang, Y., Palm, T., Grabowski, S., Montelione, G. T., and Hitchcock-Degregori, S. E. (2003) The structure of the carboxyl terminus of striated α-tropomyosin in solution reveals an unusual parallel arrangement of interacting α-helices, *Biochemistry 42*, 614−619.
32. Bacchiochi, C., Graceffa, P., and Lehrer, S. S. (2004) Myosin induced movement of αα, α*β*, and *ββ* smooth muscle tropomyosin on actin observed by multisite FRET, *Biophys. J. 86*, 2295−2307.
33. Kluwe, L., Maeda, K., Miegel, A., Fujita-Becker, S., Maeda, Y., Talbo, G., Houthaeve, T., and Kellner, R. (1995) Rabbit skeletal muscle αα-tropomyosin expressed in baculovirus-infected inect cells possesses the authentic N-terminus structure and functions, *J. Muscle Res. Cell Motil. 16*, 103−110.
34. Clos, J., and Brandau, S. (1994) pJC20 and pJC40: Two high-copy-number vectors for T7 RNA polymerase dependant expression of recombinant genes in *Eschericia coli*, *Protein Expression Purif. 5*, 133−137.
35. Kremneva, E., Nikolaeva, O., Maytum, R., Arutyunyan, A. M., Kleimenov, S. Y., Geeves, M. A., and Levitsky, D. I. (2006) Thermal unfolding of smooth muscle and nonmuscle tropomyosin α-homodimers with alternatively spliced exons, *FEBS J. 273*, 588−600.
36. Maytum, R., Lehrer, S. S., and Geeves, M. A. (1999) Cooperativity and switching within the three-state model of muscle regulation, *Biochemistry 38*, 1102−1110.
37. Potter, J. D. (1982) Preparation of troponin and its subunits, *Methods Enzymol. 85* (Part B), 241−263.
38. Malnic, B., Farah, C. S., and Reinach, F. C. (1998) Regulatory properties of the NH_2- and COOH-terminal domains of troponin T. ATPase activation and binding to troponin I and troponin C, *J. Biol. Chem. 273*, 10594−10601.
39. Weeds, A. G., and Taylor, R. S. (1975) Separation of subfragment-1 isoenzymes from rabbit skeletal muscle myosin, *Nature 257*, 54−56.
40. Spudich, J. A., and Watt, S. (1971) The regulation of rabbit skeletal muscle contraction. I. Biochemical studies of the interaction of the tropomyosin-troponin complex with actin and the proteolytic fragments of myosin, *J. Biol. Chem. 246*, 4866−4871.
41. Cooper, J. A. (1987) Effects of cytochalasin and phalloidin on actin, *J. Cell Biol. 105*, 1473−1478.
42. McKillop, D. F., and Geeves, M. A. (1993) Regulation of the interaction between actin and myosin subfragment 1: Evidence for three states of the thin filament, *Biophys. J. 65*, 693−701.
43. Vibert, P., Craig, R., and Lehman, W. (1997) Steric model for activation of muscle thin filaments, *J. Mol. Biol. 266*, 8−14.
44. Golitsina, N. L., and Lehrer, S. S. (1999) Smooth muscle α-tropomyosin crosslinks to caldesmon, to actin and to myosin subfragment 1 on the muscle thin filament, *FEBS Lett. 463*, 146−150.
45. Graceffa, P. (1989) In register homodimers of smooth muscle tropomyosin, *Biochemistry 28*, 1282−1287.
46. Paulucci, A. A., Katsuyama, A. M., Sousa, A. D., and Farah, C. S. (2004) A specific C-terminal deletion in tropomyosin results in a stronger head-to-tail interaction and increased polymerisation, *Eur. J. Biochem. 271*, 589−600.
47. Brown, J. H., Kim, K. H., Jun, G., Greenfield, N. J., Dominguez, R., Volkmann, N., Hitchcock-Degregori, S. E., and Cohen, C. (2001) Deciphering the design of the tropomyosin molecule, *Proc. Natl. Acad. Sci. U.S.A. 98*, 8496−8501.
48. Cassell, M., and Tobacman, L. S. (1996) Opposite effects of myosin subfragment 1 on binding of cardiac troponin and tropomyosin to the thin filament, *J. Biol. Chem. 271*, 12867−12872.
49. Wegner, A. (1979) Equilibrium of the actin-tropomyosin interaction, *J. Mol. Biol. 311*, 1027−1036.
50. Cho, Y. J. (2000) The carboxyl terminal amino acid residues glutamine276-threonine277 are important for actin affinity of the unacetylated smooth α-tropomyosin, *J. Biochem. Mol. Biol. 33*, 531−536.
51. Boussouff, S. E., Maytum, R., Jaquet, K., and Geeves, M. A. (2007) Role of tropomyosin isoforms in the calcium sensitivity of striated muscle thin filaments, *J. Muscle Res. Cell Motil. 28*, 49−58.
52. Maytum, R., Konrad, M., Lehrer, S. S., and Geeves, M. A. (2001) Regulatory properties of tropomyosin effects of length, isoform, and N-terminal sequence, *Biochemistry 40*, 7334−7441.

BI701144G